

Osmotic Cracking in Unsaturated Polyester Matrices Under Humid Environment

L. GAUTIER,¹ B. MORTAIGNE,¹ V. BELLENGER,² J. VERDU²

¹ DGA/DCE/CTA-16bis, avenue Prieur de la Côte d'Or-94114 Arcueil, France

² ENSAM/LTVP-151, blvd de l'Hôpital-75013 Paris, France

Received 21 October 1999; accepted 17 March 2000

ABSTRACT: Glass fiber reinforced polyester composites are widely used in marine applications where they may undergo chemical and physical aging. For this kind of laminates, the durability is governed mainly by the matrix degradation. The mechanical property reduction is not induced only by hydrolytic aging but rather by the formation of cracks or blisters. That is the reason why it became of major interest to understand the microcrack nucleation mechanism in neat matrices, to study the crack propagation, and to evaluate the incidence of cracking on the tensile property loss. We first put forward a nucleation mechanism based on polyester-organic molecule phase separation, and drew a simple kinetic model to take into account the existence of a crack induction time that is dependent on temperature and matrix structure. Crack propagation results from the build up of an osmotic pressure in microcavities, which is proportional to solute concentration. This second step has been studied in terms of crack density evolution and crack propagation rate. Finally, there is a good correlation between tensile mechanical properties variation and crack parameters. © 2001 John Wiley & Sons, Inc. *J Appl Polym Sci* 79: 2517–2526, 2001

Key words: polyester; hydrolysis; osmotic cracking; kinetic model; crack propagation

INTRODUCTION

There is a relatively abundant body of literature on the humid aging of polyester-glass fiber composites owing to their frequent use in pipes, tanks, swimming pools, and boats. Despite the very large diversity of materials and testing methods, there is a wide consensus on the fact that the durability of composites based on unsaturated polyester (UP) depends mainly on the matrix composition, for instance isophthalic systems are more stable than orthophthalic ones,¹ neopentyl glycol systems are more stable than propylene glycol ones,² and so on. These observations would

be very difficult to explain if the composite failure would be governed by the fiber or by the interface degradation. It is clear that these materials perish generally by the matrix degradation and more precisely by the hydrolytic degradation. In polymers as brittle as UP, mechanical properties are not expected to be very sensitive to chain scissions, and this can be checked by a comparison of virgin samples differing by the initial prepolymer molar mass. It is easy to understand that a UP sample based on a prepolymer of molar mass 1500 g/mol⁻¹ can be considered as a model of a UP sample based on a prepolymer of molar mass 3000 g/mol⁻¹, which has undergone one hydrolysis event per initial prepolymer chain. Despite the relatively high conversion of this hypothetical hydrolysis process, the difference between their mechanical behavior can be considered negligible.

Correspondence to: B. Mortaigne.

Journal of Applied Polymer Science, Vol. 79, 2517–2526 (2001)
© 2001 John Wiley & Sons, Inc.

In the real case of hydrolysis, however, one can observe a catastrophic change of mechanical properties due to formation of cracks and blisters, the latter being cracks that propagate preferentially parallel to the surface, below the gel-coat layer.³ It was very rapidly recognized that cracking/blistering induced by humid aging is a very important mode of failure in these materials, and that crack propagation results from the build up of osmotic pressure in microcavities, so the phenomenon was called osmotic cracking.^{4,5} Osmotic cracking requires on the one hand the presence of water in the cracks, which is not surprising in the aging conditions under study and considering the UP permeability to water,⁶ and requires on the other hand the presence of solutes in the microcrack, which was experimentally showed by several authors on blisters.^{4,7} The UP layer between a given microcavity and the bath must be semi-permeable, i.e., permeable to water and less permeable to the solutes (impermeable in the time scale under consideration). Then, according to Hoff,⁸ the osmotic pressure P must be:

$$\Pi = RT \sum_i C_i \quad (1)$$

where R is the gas constant, and C_i is the concentration of the i^{th} solute in the cavity.

Fracture mechanics allow us to predict that, above a given critical pressure Π_C , the cracks will propagate in the direction where the cavity curvature radius is the smallest.^{9,10} Indeed, in a composite material, the crack propagation direction will be determined by the mechanical anisotropy. The osmotic cracking mechanism seem to be now relatively well understood, but many important features of the process remain unclear, especially the nature of the initiation mechanism.

The purpose of this paper is to resume some recent results obtained in these domains. The first part will be devoted to a kinetic study of the onset of cracking, leading to the notion of induction time. Taking the experimental result into account, we put forward a crack initiation mechanism, and a kinetic model as well as the experimental checking of various assumptions. The last part of the paper will focus on the consequence of crack propagation on tensile mechanical properties.

EXPERIMENTAL

Most of the experimental results reported in this paper were obtained with two resins: resin A, a

classical resin with isophthalic/maleic (1/1) acids and propylene glycol cross-linked by 45% of styrene, and resin B, orthophthalic/maleic acids with a mixture of glycols (ethylene glycol, propylene glycol, and diethylene glycol) modified by dicyclopentadiene (DCPD) in order to reduce styrene emission (styrene mass fraction 34%). The same initiating system (1.2% methylethylketone peroxide + 0.5% cobalt octoate) and the same curing process (24 h at room temperature + 10 h at 80°C and 4 h at 120°C) were used for both resins. Aging tests were made on discs of 32 mm diameter, 1 mm thickness, and polished in order to enable optical tests. The samples are first vacuum dried for 1 week at 50°C prior to immersion in water at 30, 50, 70, and 100°C. Weight changes are recorded periodically on a 10^{-4} precision balance.

Samples are observed with a NIKON optical microscope. The Young modulus (E), the stress (σ) and the strain (ϵ) at break are measured on an tensile INSTRON 6025 at a constant rate of 1 mm/min at room temperature.

RESULTS AND DISCUSSION

Onset of Cracking

In sufficiently thin samples (typically thinner than 1 mm) and at sufficiently low temperature (typically < 100°C) cracking is not diffusion controlled. Water uptake reached a plateau corresponding to the sorption equilibrium and the osmotic cracking corresponds to a mass re-increase after a more or less long induction period. The cracks grow until the point where they coalesce and form an open network. Thus the mass re-decreases rapidly because most of the molecules trapped inside the network leach in the bath because of their high solubility in water. In mass curves, it can be in principle considered that the onset of mass re-increase corresponds to the induction time of osmotic cracking t_i . Relationships between t_i and the network structure and composition can be used to establish the osmosis causes.¹¹

The kinetic curves of mass changes during immersion in distilled water at 100°C and 70°C of samples A and B are shown in Figure 1.

At 100°C, the onset of mass re-increase occurs very early for both matrices (24 h for A and 6 h for B) and is followed by a sharp weight loss that appears after 10 h for B and 400 h for A. At 70°C, no weight changes are recorded for the A sample.

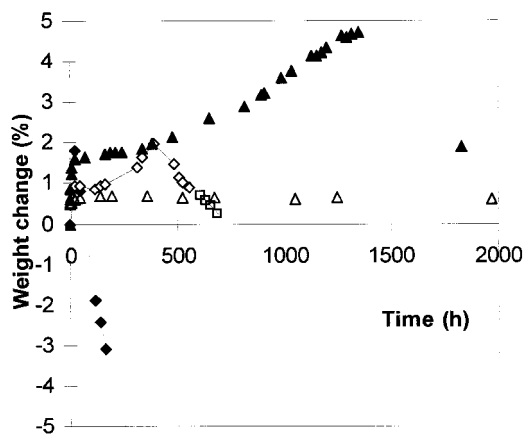


Figure 1 Observed net weight changes of matrices A (white symbol) and B (black symbol) immersed in water at 100°C (◆) and 70°C (▲).

As for sample B, the induction time of cracking (onset of mass re-increase) could be located between 100 and 300 h depending on the chosen criterion, whereas the characteristic time of diffusion t_D taken at the intersection of the tangent at origin with the equilibrium plateau is about 5 h. The mass uptake goes from 1.6% to 5% between 500 and 1500 h, which means that, at 1500 h, the volume fraction of cracks is about 3.5%.

Disk-shaped microcracks with radial lines or ellipsoidal cracks are also observed using an optical microscope (Fig. 2). It has been arbitrarily chosen to consider that the induction period ends when the crack diameter reached the critical value of 40 μm . The corresponding induction time t_{ind} is about 70 h for sample B, compared with 100–300 h from gravimetric experiments. Indeed,

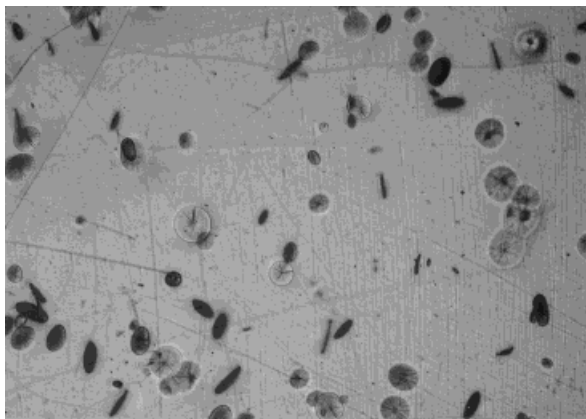


Figure 2 Disk-shaped and ellipsoidal cracks in polyester resin after immersion in water.

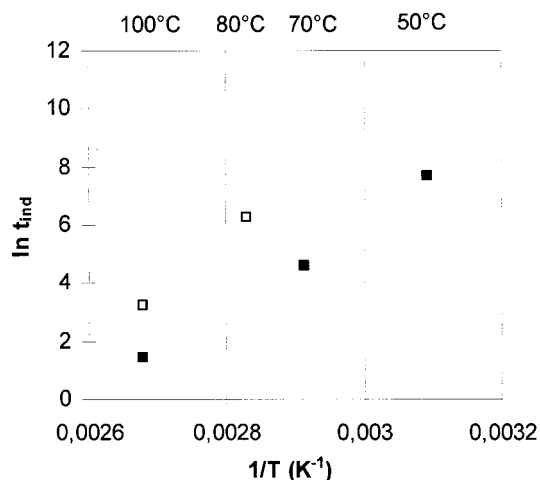


Figure 3 Arrhenius plots of t_{ind} for matrices A (□) and B (■).

the relative sensitivities of microscopic and gravimetric detections of the onset of cracking depend of the crack density N (number of cracks per volume unit). Schematically gravimetric analysis cannot detect situations such as:

$$N\nu \leq \left(\frac{\Delta m}{m}\right)_0 \quad (2)$$

where $\left(\frac{\Delta m}{m}\right)_0$ is the sensitivity threshold of gravimetric measurements, typically of the order of 10^{-3} , and ν is the average volume of a crack. An arrhenius plot of induction times t_{ind} determined by microscopy is presented in Figure 3.

In sample A, no cracking was observed at 70°C after a 10 000-h exposure, explaining the positive curvature of the curve. For sample B, which is considerably less stable, the induction time has been determined also at 50°C. The curve also displays a positive curvature that could be due to the fact that the networks are in the rubbery state in the left part of the curve and in the glassy state in the right part in the range of temperature studied ($T_{gA} = 96^\circ\text{C}$, $T_{gB} = 82^\circ\text{C}$).

Crack Initiation Mechanism and Kinetics

There are generally two ways in the literature to explain the initiation of osmotic cracks:

1. Heterogeneity pre-exists in the network. They may be microporosities induced by air bubbles, soluble impurities, or defects. This

approach is somewhat difficult to reconcile with the numerous observations showing a strong influence of the network structure on the induction time, as for instance, in the above presented results. In the case of long induction periods, it is clear that the crack nucleation is the rate controlling process. Authors such as Robeson and Crisafulli¹² have suggested that heterogeneity formation (cluster) could be inherent to the sorption process, but in this case water diffusion should mask such effects.

2. Crack initiation results from a polymer-water demixing. This mechanism has been well established in the cases where saturated samples are quenched. Because in these polymers the equilibrium concentration is an increasing function of temperature, quenched samples are over-saturated and phase separation occurs.¹³ For Lee et al.,¹⁴ aging would have the same effect as quenching, meaning that aging would shift the equilibrium towards lower water concentration. This interpretation contradicts the experimental results that reveal that hydrophilicity increases during hydrolytic aging.¹⁵ Furthermore, aging is sufficiently slow (at least in a thin sample) to be not kinetically controlled by water diffusion. Thus, the latter should easily eliminate any aging induced by spatial fluctuation of the water concentration in the timescale of aging tests.

Because these mechanisms are not satisfying, there remains only one possibility: that crack initiation is linked to the presence of small water-soluble molecules present in the network. These molecules would accumulate as a result of their formation from polymer hydrolysis and they will phase separate when exceeding their equilibrium concentration, thus creating highly hydrophilic liquid micropockets able to initiate osmotic cracking.

This theory displays many advantages over former ones: first, it is consistent with the structure—durability experimental relationships (see below). Second, it can explain the delayed character of osmotic cracking in relatively stable samples.

The hypothesis inherent to this theory will be discussed in the next part of this paper. The hypothesis being made, the theory must take into account apparently independent factors, such as

the effect of initially present impurities (catalytic residues, unreacted monomers,⁷ dangling chains,¹⁶ and network structure.¹⁷ These factors can be integrated to a simple kinetic model based on the following assumptions:

1. Hydrolysis can be described by the standard second order kinetic scheme where ester groups are randomly attacked by water.¹
2. In a first approach, the reaction is not diffusion controlled (sample thickness of the order of 1 mm) but the theory can be easily extended to the diffusion controlled case.
3. There is only one water-soluble cracking promoting species, for instance monomeric glycols. This is a reasonable assumption in that phthalic acids are not very soluble in water. Anyway, the existence of many distinct species would modify only quantitatively the model.
4. Water equilibrium concentration does not vary with hydrolysis conversion. In fact, it increases slowly but its variation can be neglected in a first approach.

Then, the hydrolysis rate can be ascribed:

$$\frac{dn}{dt} = kEW \approx KE_0 \quad (3)$$

where n , E , and W are the respective number of chain scission per mass unit, ester concentration, and water concentration, k being the second order constant, $K = kW$ being a pseudo first order constant, and $E = E_0 - n \approx E_0$ at low conversions.

Each hydrolysis event creates two new dangling chains. If a hydrolysis event occurs near a chain end, it generates a small organic molecule. In a first approximation, the rate of small molecule formation is then:

$$\frac{d\gamma}{dt} = 2k\varphi Wn = 2\varphi Kn \quad (4)$$

where γ is the number of small molecule per mass unit and φ is the number of reactive ester groups in a dangling chain (close to unity).

The small molecules are supposed to have a very low transport rate in the polymer, so that their loss by diffusion is neglected.

The integration of the eq. (3) gives:

Table I Intrinsic Parameters

Matrix	γ_0 (10^6 mol/g $^{-1}$)	n_0 (10^4 mol/g $^{-1}$)	E_0 (10^4 mol/g $^{-1}$)
A	1.3	8.2	60
B	14.0	13.1	64

$$n = n_0 + KE_0t \quad (5)$$

where n_0 is the initial number of “chain scissions,” i.e., half the number of dangling chains. And, substituting n in eq. (4) gives:

$$\gamma = \gamma_0 + 2\varphi Kn_0t + \varphi K^2 E_0 t^2 \quad (6)$$

The first term corresponds to the initially present water-soluble small molecules.

The second term refers to the small molecules generated by chain scissions on initially present dangling chains.

The third term is attributed to the small organic molecules generated by chain scissions in dangling chains resulting from hydrolysis events in initially elastically active network chains.

Demixing is supposed to occur at constant molecules concentration γ_C , at least in a first approach, so that the induction time t_{ind} would be the solution of the following second order equation:

$$\varphi K^2 E_0 t^2 + 2\varphi Kn_0t - (\gamma_C - \gamma_0) = 0 \quad (7)$$

whose solution is:

$$t_{\text{ind}} = \frac{n_0}{KE_0} \left\{ \left[1 + \frac{E_0(\gamma_C - \gamma_0)}{\varphi n_0^2} \right]^{1/2} - 1 \right\} \quad (8)$$

The effect of initially present molecules is well put in evidence: for $\gamma_0 \geq \gamma_C$, $t_{\text{ind}} = 0$. In the case of high initial dangling chains concentration, typically for

$$n_0 \geq \sqrt{\frac{5}{\varphi}} [E_0(\gamma_C - \gamma_0)]^{1/2} \quad (9)$$

we would have:

$$t_{\text{ind}} \approx \frac{n_0}{2KE_0} \frac{E_0(\gamma_C - \gamma_0)}{\varphi n_0^2} \approx \frac{1}{2K} \frac{\gamma_C - \gamma_0}{n_0} \quad (10)$$

In other words, the induction time would be inversely proportional to the initial dangling chain concentration.

Finally, the induction time value is proportional to the reciprocal of the rate constant K , which represents the intrinsic hydrolytic stability of ester functions.

A detailed analysis based on statistical considerations and chemical characterization¹⁵ of matrices A and B gave the following results presented in Table I.

The pseudo first order constant K has been determined using spectrometric analysis as reported by Belan et al.¹⁵ (see Table II).

To conclude, the difference of stability between the matrices A and B can be explained by this model, which opens the way to lifetime prediction from initial analytical data and structure-reactivity relationships provided that γ_C , the equilibrium concentration of small molecule, is known. At 70°C, the cracking resistance of sample A is explained by its hydrolytic stability (very low value of K) whereas at 100°C, the high value of γ_0 and n_0 explain the relative difference between the two matrices observed in Figure 1.

Model Experimental Checking

Two assumptions have to be checked:

1. The matrix acts as a semipermeable membrane, i.e., the permeability of small organic molecules, suspected to play a key role in osmotic pressure build up, especially glycols, is many orders of magnitudes lower than water permeability. This is well established by water and glycol sorption kinetics comparison.
2. Small molecules promote osmotic cracking. We have incorporated various propylene glycol weight fraction into reactive mixtures A and B, below the equilibrium threshold, which means that the sample remains initially homogeneous. Then the

Table II Pseudo First Order Constant Values

Matrix	Temperature (°C)	K (10^5 h $^{-1}$)
A	100	35.0
B	100	13.0
B	70	3.8
B	50	1.0

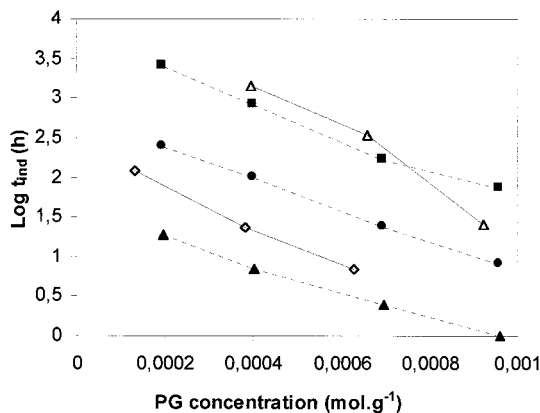


Figure 4 Influence of added propylene glycol on crack induction time in sample A (white symbol) and B (black symbol) as a function of temperature: 80°C (◆), 70°C (▲), 50°C (●), 30°C (■).

samples were cured and exposed to immersion at various temperatures. The induction time was determined by microscopic observations and plotted against glycol concentration in Figure 4.

The induction time displays an exponential dependence with the glycol concentration.

$$\log t_{ind} = \log t_0 - B[PG] \quad (11)$$

The parameter values are given in Table III.

As a conclusion, the addition of various concentration of PG influences the induction time according to the following function:

$$t = t_0^{-B[PG]} \quad (12)$$

where B is almost temperature independent, whereas t_0 increases when the temperature decreases.

Table III Parameters of the Crack Induction Time Law

System	Temperature (°C)	B (h · g/mol ⁻¹)	Log t_0 (h)
A	80	2500	2.37
A	70	2950	4.38
B	70	1650	1.56
B	50	1960	2.78
B	30	2050	3.76

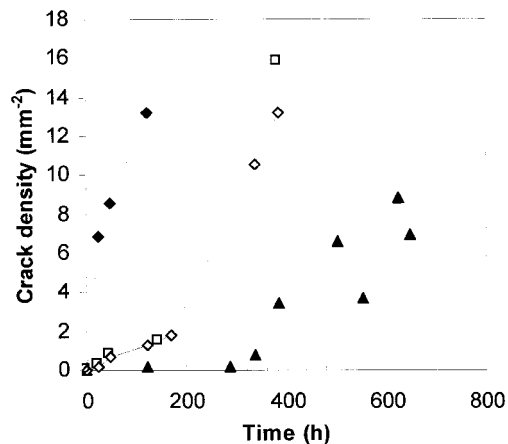


Figure 5 Crack density evolution in matrices A (white symbol) and B (black symbol) at 100°C (◆) and 70°C (▲).

The induction time t_0 corresponds to the case where no PG were artificially added.

Crack Propagation

Once the nucleation site has been formed, the propagation step can take place. The main characteristics of this crack propagation are the crack propagation rate and the crack density evolution. As a matter of fact, the propagation seems to proceed by a nucleation/spreading mode, meaning that both crack density and crack size increase during hydrothermal aging. Both were determined using optical observations.

The results for the materials under investigation are shown in Figures 5 and 6. The crack

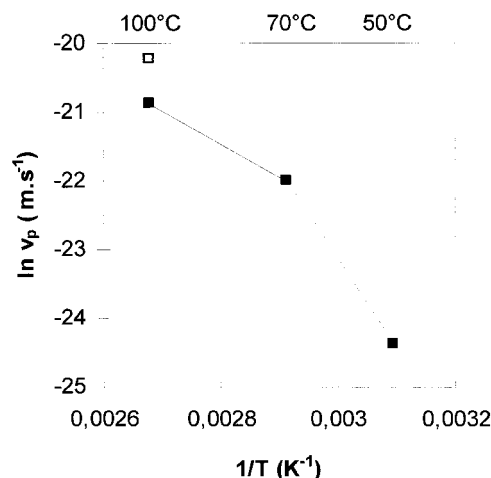


Figure 6 Arrhenius plot of the crack propagation rate in matrices A (□) and B (■).

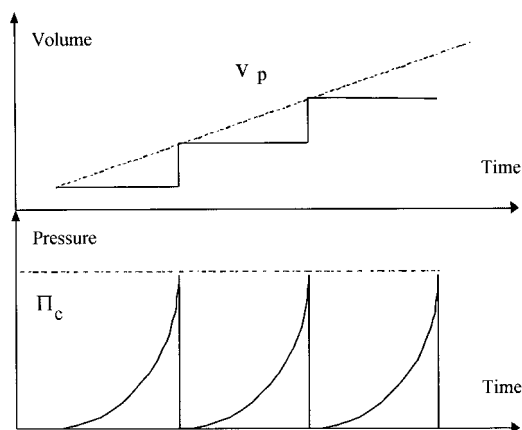


Figure 7 Crack propagation mechanism.

density evolution has been put in parallel with gravimetric curves. The low crack density evolution in sample A before 200 h may explain why a mass uptake is not visible before 200 h, whereas the number of cracks in sample B increases rapidly as soon as crack initiation occurs. At 100°C, the matrix A exhibits a slightly higher propagation rate. This rate is a thermo-activated phenomenon.

Propagation results can be interpreted in terms of osmotic process and can be schemed as shown in Figure 7.

The increase of osmotic pressure Π is due to the accumulation of solute inside the micropocket, according to eq. (1). At a critical value Π_c the microcrack size increases, thus leading to the decrease of solute concentration and therefore to the osmotic pressure. This pressure drop stabilizes the micropocket size until the osmotic pressure reaches Π_c by increase of solute concentration. The cavity volume evolution corresponds to the minimum energy loss and is found to depend on the square root of the solute mole number.⁹ This mechanism is in accordance with the slip/stick propagation mode that can be observed on the crack surface.¹⁰ This step ends when the cracks coalesce to the surface leading to the leaching of the free molecules.

As can be seen on Figure 7, the crack propagation rate V_p is governed by two parameters: the molecule production rate and the critical pressure at which the micropocket size increases. The first parameter depends on the chemical hydrolysis kinetics described earlier and noted γ . It is clearly dependent on the pseudo first order constant K . The values in Table III had shown the same hierarchy ($K_A < K_B$).

The critical pressure Π_c has been determined according to linear elastic fracture mechanics.⁹

$$\Pi_c = \left(\frac{3\zeta E}{2b} \right)^{1/2} \quad (13)$$

where E is the Young modulus, ζ is the surface energy, and b is the crack length.

It is difficult, however, to evaluate the E and ζ values in the conditions under study (at 100°C and in humid environment). As a matter of fact, those values are dependent on plasticization and temperature.

An other way to determine the Π_c value is to used the relations applied in solvent crazing process,¹⁸ namely:

$$\Pi_c = \frac{2\zeta}{r} + \frac{2\sigma_e}{3}\psi \quad (14)$$

where r is the cavity radius, σ_e is the yield stress, and ψ is a constant of the order of unity. The same incertitude on ζ value appears, but one can be sure that the yield stress decreases to a near zero value when the temperature reached the glass transition temperature. At $T > T_g$, the critical pressure is expressed by:

$$p = \frac{2\gamma}{r} \quad (15)$$

and the failure energy is then only linked to the intermolecular forces represented by the surface energy.

This approach enables us to explain why the crack propagation rate does not follow an Arrhenius law. However, no absolute critical pressure value can be calculated.

Tensile Mechanical Properties

The tensile test has been chosen to characterize the material resistance evolution as a function of immersion time in water. It appears that the Young modulus remains almost constant over aging, whereas failure properties decrease very sharply at 100°C and 70°C. Figures 8 and 9 only shows the evolution of the stress at break, but let us remember that the evolution of the strain at break follows the same tendency.

Tensile property reduction occurs in both matrices at 100°C, but only in matrix B at 70°C.

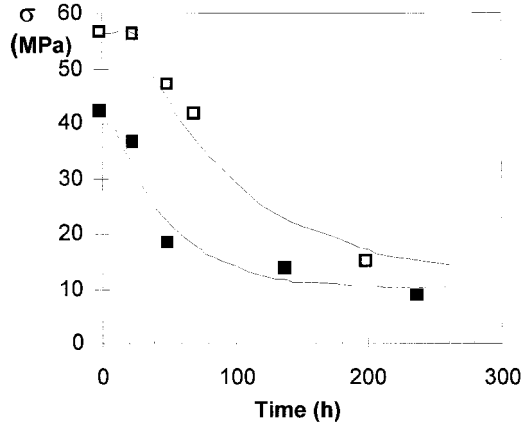


Figure 8 Stress at break evolution of matrices A (□) and B (■) as a function of immersion time at 100°C.

Hydrolytic aging of matrix A at 70°C does not have a great impact on mechanical properties. This result can be put in parallel with crack initiation ones. Osmotic damage does not appear in matrix A at 700°C on the time-scale under study. Moreover, observing Figures 8 and 9 put in evidence the existence of an induction time where failure properties remain unchanged. These observations lead us to the following equation:

$$\sigma(t) = (\sigma_0 - \sigma_\infty) \exp\left(\frac{-(t - t_r)}{\tau}\right) + \sigma_\infty \quad (16)$$

where σ , σ_0 , and σ_∞ represent respectively the stress at break at time t , initially and at an infinite time, τ is the characteristic time of tensile properties degradation, and t_r is the delay time.

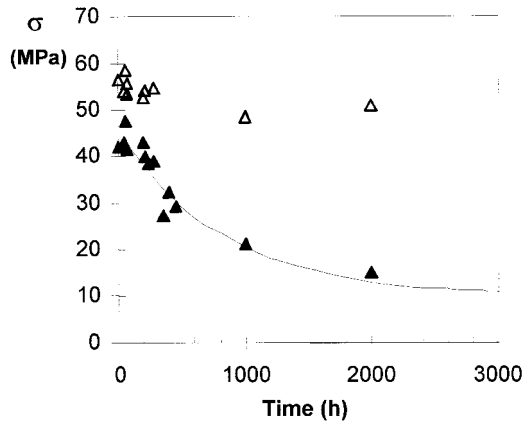


Figure 9 Stress at break evolution of matrices A (□) and B (■) as a function of immersion time at 70°C.

Table IV Parameters of the Tensile Mechanical Property Evolution

Matrix	Temperature (°C)	σ_0 (MPa)	σ_∞ (MPa)	τ (h)	t_r (h)	t_{ind} (h)
A	100	56.5	12	80	24	24
B	100	42.0	10	45	6	6
B	70	42.0	10	800	100	75

The value of σ_∞ is attributed to the asymptotic value at 100°C. The curve is then fitted by adjusting the parameters τ and t_r . The parameters are summarized in Table IV.

By comparing the delay time and the induction time, we can draw the conclusion that the onset of a decrease in tensile properties is governed by the onset of osmotic cracking. The matrix failure would therefore take place in the osmotic induced cracks.

Let us now try to understand the reason for the tensile property decrease. The usual approach is to correlate mechanical property evolution with weight changes.¹⁹ The result of such an approach is shown in Figure 10.

In all cases, a large stress at break variation is observed for a small weight loss. Thus a weight loss increase does not have a great effect on mechanical properties variation. This can be explained by the fact that weight loss becomes significant only when the crack system reaches the percolation threshold, thus leading to molecule leaching, which contributes to weight loss. The correlation does not take therefore into account the contribution of small isolated cracks. We then

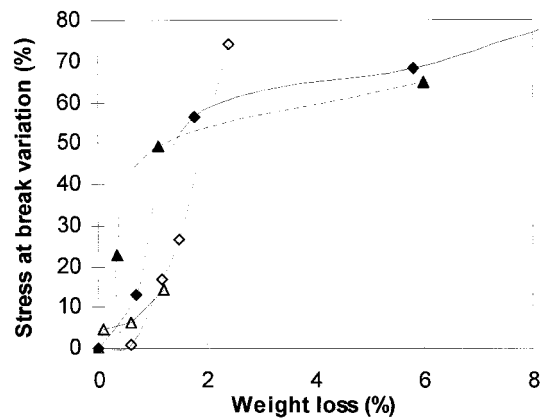


Figure 10 Stress at break variation vs weight loss at 100°C (◆) and 70°C (▲) for matrices A (white symbol) and B (black symbol).

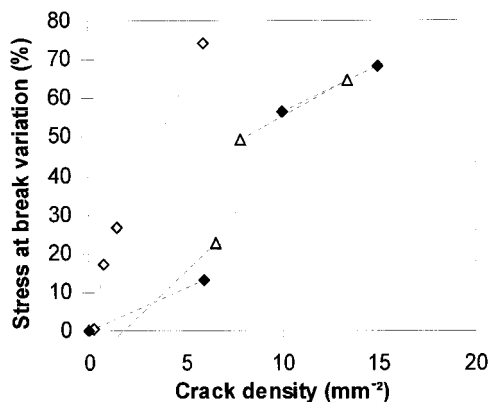


Figure 11 Stress at break variation versus crack density at 100°C (◆) and 70°C (▲) for matrices A (white symbol) and B (black symbol).

aimed at comparing mechanical property reduction with crack propagation parameter evolution, namely crack density and crack length (Figs. 11 and 12).

According to these figures, the correlation is quite good and can be explained in terms of fracture mechanics.

The Griffith criterion enables to determine the stress at break of a material containing an ellipsoidal crack of length $2c$:

$$\sigma = \left(\frac{2sE}{\pi c} \right)^{1/2} \quad (17)$$

The stress at break would therefore be proportional to the reciprocal of the square root of the crack length. As a conclusion, the stress at break variation would be governed by the crack length evolution.

CONCLUSION

Although glass fiber reinforced polymer laminates have received tremendous attention as structural materials due to their attractive weight-to-strength ratio, their mechanical properties are likely to be reduced by a chemically aggressive environment. The lack of long-term behavior information is the main limitation of their use. When polyester is used as the organic matrix, many research works have provided fundamental results showing matrix degradation as being the main parameter governing the laminate durability.

In this work, we have investigated the degradation behavior of two polyester matrices as a function of immersion time in water at different temperatures. The formation of disk-shaped or ellipsoidal cracks has been observed in the samples after a given time called induction time. Taking into account the kinetic aspects of the crack nucleation leads us to the proposal of a new crack initiation mechanism based on a polyester-small molecules phase separation. The crack nucleation promoting molecules are essentially glycols that accumulate in the network as a result of hydrolytic chain scissions. This mechanism has been experimentally validated by adding artificially glycol molecules in the network. It turned out that the induction time is reduced when a high glycol fraction is incorporated. A kinetic model has been put forward to estimate the evolution of small molecules in the network. Structural network parameters promoting crack initiation have therefore been put forward: high initially present molecule concentration, high concentration of initially present dangling chains, and high ester reactivity. This model enables us to explain the difference of water resistance in both matrices under study.

Once the micropocket has been initiated, the cavity size increases according to an osmotic process. The crack propagation proceeds by a nucleation/spreading mechanism, meaning that both crack density and crack length increase. The main characteristic of crack propagation is the crack propagation rate that is governed by the molecule production rate and the critical osmotic pressure required for the crack to propagate. These parameters explain the difference observed in the propagation rates of the matrices.

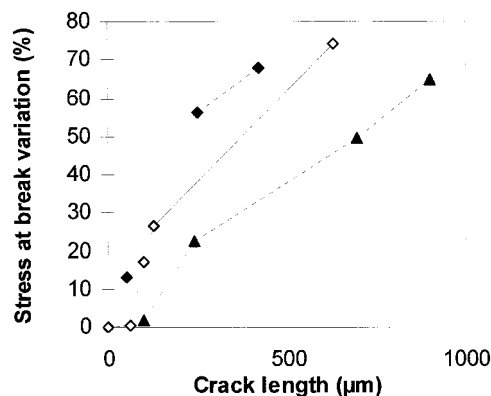


Figure 12 Stress at break variation versus crack length at 100°C (◆) and 70°C (▲) for matrices A (white symbol) and B (black symbol).

Finally, tensile analysis have provided fundamental insight into matrix degradation. Mechanical properties are not sensitive to chain scission, but the onset of osmotic cracking and its propagation have a great impact on the matrix resistance. The crack length was found to govern the tensile mechanical property reduction.

REFERENCES

1. Belan, F.; Bellenger, V.; Mortaigne, B.; Verdu, J. *Polym Deg Stab* 1997, 56, 301.
2. Curry, B. 42nd annual conference, Composites Inst., 15-A, 1987.
3. Ghotra, J. S.; Pritchard, G. *Elsevier Applied Science*, 3, 1984.
4. Ashbee, K. H. G.; Franck, F. L.; Wyatt, R. C. *Proc Roy Soc* 1967, A300, 415.
5. Ashbee, K. H. G.; Wyatt, R. C. *Proc Roy Soc* 1969, A312, 553.
6. Bellenger, V.; Mortaigne, B.; Verdu, J. *J Appl Polym Sci* 1990, 41, 1225.
7. Abeyasinghe, H. P.; Ghotra, J. S.; Pritchard, G. *Composites* 1983, January, 57.
8. Hoff, J. V. T. *Phil Mag* 1982, 36, 2662.
9. Walter, E.; Ashbee, K. H. G. *Composites* 1982, October, 365.
10. Sargent, J. P.; Ashbee, J. H. G. *J Appl Polym Sci* 1984, 29, 809.
11. Abeyasinghe, H. P.; Edwards, W. *Polymer* 1982, 23, 1785.
12. Robeson, L. M.; Crisafulli, S. T. *J Appl Polym Sci* 1983, 28, 2925.
13. Narkis, M.; Bell, J. P. *J Appl Polym Sci* 1982, 27, 2809.
14. Lee, S. B.; Rockett, T. J.; Hoffman, R. D. *Polymer* 1992, 33, 2353.
15. Belan, F.; Bellenger, V.; Mortaigne, B. *Polym Deg Stab* 1997, 56, 93.
16. Mortaigne, B.; Bellenger, V.; Verdu, J. *Polym Networks Blends* 1992, 2, 187.
17. Bellenger, V.; Mortaigne, B.; Grenier-Loustalot, M. F.; Verdu, J. *J Appl Polym Sci* 1992, 44, 643.
18. Andrews, E. H.; Bevan, L. *Polymer* 1972, 13, 337.
19. Morii, T.; Tanimoto, T.; Hamada, H.; Maekawa, Z.; Hirano, T.; Kiyosumi, K. *Polym Polym Composites* 1993, 1, 37.